here, microwave output power was measured before and after the long duration stress, and is shown in Fig. 2. As can be seen from Fig. 2, the microwave output power reduced by 3.73 dB from 1.45 to 0.61 W/mm after stress. Therefore, we observe a direct correlation between the surface charge accumulation and the microwave output power. In opposition to the short duration stress effects that disappear after some time or under UV illumination [5], the effects of the long duration stress is permanent and unaffected by UV illumination [7]. These results clearly point out the degradation of unpassivated AlGaN/GaN HEMTs when subjected to long duration electrical bias stress.

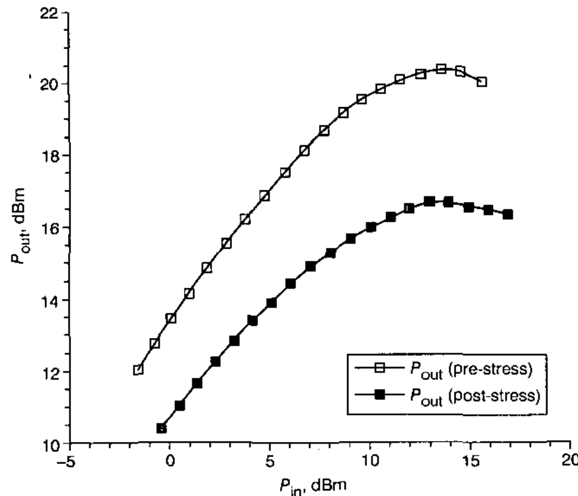

Fig. 2 *Microwave output power measured at 4 GHz before and after long duration stress at $V_d = 15$ V and $V_g = -5$ V*

Conclusions: We have studied the effects of long duration electrical bias stress on AlGaN/GaN HEMTs. We have observed that the surface potential and drain current transient magnitudes increase dramatically after stress, indicating a larger accumulation of negative charges near the gate after stress. The microwave output power also decreases dramatically after stress in direct correlation with the increased drain current and surface potential transient magnitudes. It is possible that some permanent changes in the gate Schottky contact or surface electronic properties are caused by the stress that result in such a degradation in device performance.

Acknowledgments: The authors would like to acknowledge J. Smart and J.R. Shealy for AlGaN/GaN heterostructure samples, and V. Tilak for help with HEMT device fabrication. This work is supported by the Office of Naval Research MURI on semiconductor interface electronics under Contract No. N00014-99-1-0714 under the direction of C.E.C. Wood.

© IEE 2003
7 June 2003
Electronics Letters Online No: 20030773
DOI: 10.1049/el:20030773

G. Koley, H. Kim, L.F. Eastman and M.G. Spencer (*School of Electrical and Computer Engineering, Cornell University, Ithaca, New York 14853, USA*)

E-mail: gk33@cornell.edu

References

1 EASTMAN, L.F., TILAK, V., SMART, J., GREEN, B.M., CHUMBES, E.M., DIMITROV, R., KIM, H., AMBACHER, O., WEIMANN, N., PRUNTY, T., MURPHY, M., SCHAFF, W.J., and SHEALY, J.R.: 'Undoped AlGaN/GaN HEMTs for microwave power amplification', *IEEE Trans. Electron Devices*, 2001, **48**, (3), pp. 479–485

2 KELLER, S., WU, Y., PARISH, G., ZIANG, N., XU, J.J., KELLER, B.P., DENBAARS, S.P., and MISHRA, U.K.: 'Gallium nitride based high power heterojunction field effect transistors: process development and present status at UCSB', *IEEE Trans. Electron Devices*, 2001, **48**, (3), pp. 552–559

3 VETURY, R., ZHANG, N.Q., KELLER, S., and MISHRA, U.K.: 'The impact of surface states on the DC and RF characteristics of AlGaN/GaN HFETs', *IEEE Trans. Electron Devices*, 2001, **48**, (3), pp. 560–566

4 GREEN, B.M., CHU, K.K., CHUMBES, E.M., SMART, J.A., SHEALY, J.R., and EASTMAN, L.F.: 'The effect of surface passivation on the microwave characteristics of undoped AlGaN/GaN HEMTs', *IEEE Electron Device Lett.*, 2000, **21**, (6), pp. 268–270

5 KOLEY, G., TILAK, V., EASTMAN, L.F., and SPENCER, M.G.: 'Slow transients observed in AlGaN/GaN HFETs: effects of SiN_x passivation and UV illumination', *IEEE Trans. Electron Devices*, 2003 (to be published)

6 KOLEY, G., and SPENCER, M.G.: 'Surface potential measurements on GaN and AlGaN/GaN heterostructures by scanning Kelvin probe microscopy', *J. Appl. Phys.*, 2001, **90**, (1), pp. 337–344

7 KIM, H., THOMPSON, R.M., TILAK, V., PRUNTY, T.R., SHEALY, J.R., and EASTMAN, L.F.: 'Effects of SiN passivation and high electric field on AlGaN/GaN HFET degradation', *IEEE Electron Device Lett.*, 2003 (to be published)

SiGe power devices for 802.11a wireless LAN applications at 5 GHz

A. Keerti and A. Pham

The feasibility of SiGe heterojunction bipolar transistors (HBTs) for 802.11a wireless LAN power amplifier applications in the 5 GHz regime is demonstrated. The device layout is optimised using unit power devices to develop high-power HBTs. SiGe HBTs with an emitter area of 1152 μm^2 achieve a maximum output power of 25 dBm and PAE of 36% at 5.35 GHz under a supply voltage of 3.0 V. The measured ACPR for this device under OFDM modulated signal is −23 and −32 dBc at 10 and 20 MHz offset, respectively, at an output power backed off by 9 dB from P_{1dB}.

Introduction: The wireless local area network (WLAN) market has grown at a very rapid pace for the past several years. The 802.11 WLAN standards have evolved from 2.4 to 5 GHz bands to increase the rate of data transmission. The new generation of 802.11a WLAN and HiperLAN2 standards operating in the 5 GHz spectrum using orthogonal frequency division multiplexing (OFDM) [1] are becoming popular due to high speed, greater system capacity, low interference and less congestion. Typically, the required power level for the 802.11a standard in 5.15–5.25 GHz, 5.25–5.35 GHz and 5.75–5.85 GHz bands is 50, 250 mW and 1 W, respectively [2]. Traditionally, III–V compound semiconductor technologies such as GaAs, InP have been the prime candidate for meeting RF power and efficiency requirements. However, RF Si ICs have recently demonstrated their competitive advantages for WLAN applications [3–5]. Recently, SiGe HBT power amplifiers have been demonstrated for 802.11b applications at 2.4 GHz [6–9] and are emerging as a contender for RF power amplifier applications at higher frequencies. In this Letter, we report the full characterisation of SiGe HBTs at 5 GHz in terms of maximum output power, power-added efficiency and linearity. The experimental results demonstrate that the RF SiGe process can be used for power amplifier applications in the 5 GHz regime.

Technology and layout: The power HBTs are fabricated in Austria Microsystems (AMS) 0.8 μm SiGe process, fully compatible with CMOS for complex high-speed system-level integration [10]. This is a two-metal, three-poly production qualified process featuring high-speed and low-noise heterojunction transistors having graded Ge profile in base, CMOS transistors, very low-parasitic linear capacitors, linear resistors and spiral inductors.

The layout of a power HBT at radio frequencies is important considering the desired high power level and temperature effects. A multiple emitter finger distribution technique is used to optimise the layout of large RF transistors. This configuration provides high current density and reduces the lateral current crowding affects. It also reduces the base resistance and junction parasitic effects resulting in better f_T and f_{max} [11]. In this layout, four emitter fingers with optimised finger width of 0.8 μm and finger length of 30 μm are used to form a single unit cell. The unit device has peak $f_T = 35$ GHz, peak $f_{max} = 40$ GHz, $V_{CBO} = 14$ V, $V_{CEO} = 4.5$ V and $V_A = 100$ V. The unit devices are connected in parallel, in a matrix type of structure consisting of four columns each having six unit cells to realise a power transistor having

emitter area 1152 μm². This ensures uniform current distribution and can reduce thermal runaway. Substrate contacts are placed around each unit cell to minimise the substrate losses [12]. The advantage of two metal layers as signal feed lines allows proper base, collector and emitter connections with minimum parasitics. Fig. 1 shows the layout of the unit cell and a picture of the fabricated HBT device.

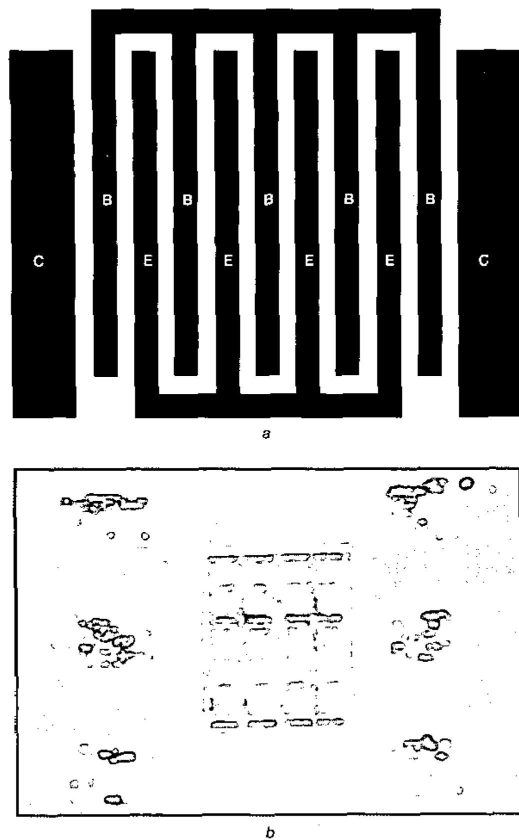

Fig. 1 *Layout of unit cell and picture of HBTs in 0.8 μm SiGe AMS process*
a Layout of unit cell
b Picture of HBTs

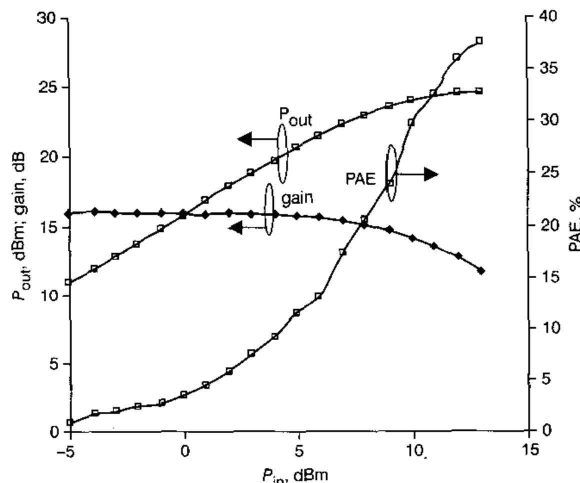

Fig. 2 *Measured P_{out}, gain and PAE for device of emitter area 1152 μm² at 3 V bias*

Large signal performance: The power devices are tested on-wafer at 5.35 GHz using the Maury Microwave load-pull measurement system. All the devices are biased at $V_{BE} = 0.85$ V and collector bias $V_{CE} =$ 3.0 V. A pre-match tuning technique is employed to match the input of the devices. Source and load matching networks are optimised for maximum output power with source reflection coefficient of magnitude 0.6715 and phase −176.74° and load reflection coefficient of magnitude 0.7653 and phase 177.4°. Fig. 2 shows the RF characteristics of a large transistor with emitter area of 1152 μm² under a single tone CW signal. This transistor delivers a maximum RF output power of 25 dBm, making it suitable for 802.11a WLAN applications. It exhibits a linear gain of 15.4 dB and maximum power-added efficiency (PAE) of 36%. The gain variation is <1.6 dB while PAE remains above 33% as collector bias is varied from 2.5 to 3.3 V as shown in Fig. 3. The power spectrum shown in Fig. 4 is for the same HBT device stimulated by OFDM modulated 802.11a WLAN signal. Agilent's vector signal generator ESG 4358C is used to generate the OFDM modulated signal at 5.35 GHz and 64-level quadrature amplitude modulation (64QAM) is employed to achieve the 54 Mbit/s data rate. In dense multicarrier communication systems, the envelope-modulated signals have high peak-to-average ratios due to random occurrence of high peaks. To keep the intermodulation distortion to acceptable levels, the peak envelope power is made to swing up to P_{1dB} which results in back off of average output power. In OFDM, the high peak-to-average ratio postulates a 9 dB back off from P_{1dB}. The measured adjacent channel power ratio (ACPR) at 10 and 20 MHz offset is −23 and −32 dBc, respectively, which meets the spectral mask requirement of the standard.

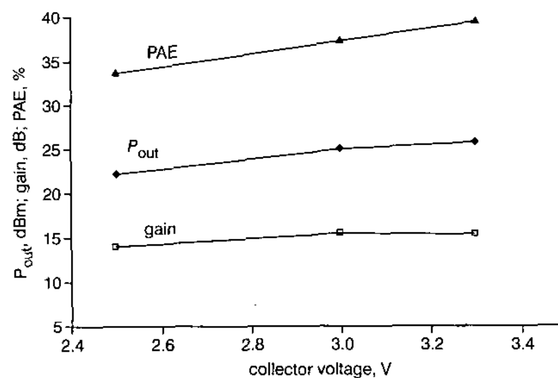

Fig. 3 *Measured P_{out}, gain and PAE against collector bias*

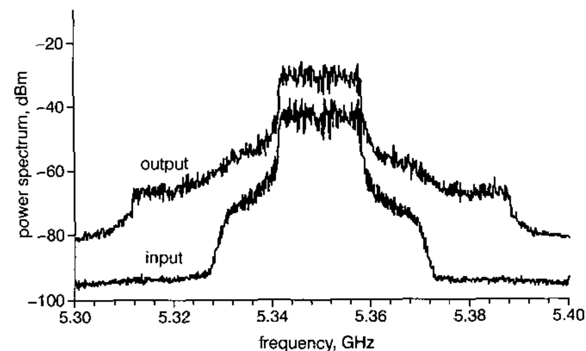

Fig. 4 *Power spectrum of SiGe HBT under OFDM modulated 802.11a signal*

Conclusion: The feasibility of SiGe HBTs for WLAN applications has been demonstrated. A maximum output power of 25 dBm and PAE of 36% at 5.35 GHz with 3 V supply is achieved for an SiGe HBT with emitter area of 1152 μm² by optimisation of the layout. The measured ACPR for the SiGe HBT under OFDM modulated signal met the spectral mask requirements of the 802.11a WLAN standard. The performance of these devices demonstrates the viability of SiGe integrated circuits for power amplifier applications in the 5 GHz regime.

© IEE 2003 *16 April 2003*
Electronics Letters Online No: 20030764
DOI: 10.1049/el:20030764

A. Keerti and A. Pham (*Microwave Microsystems Laboratory, University of California, Department of Electrical and Computer Engineering, Davis, CA 95616, USA*)

References

1 IEEE Draft Supplement to IEEE Standard 802.11: 'Wireless LAN Medium Access Control (MAC) and Physical Layer (PHY) Specifications: High-speed Physical Layer in the 5 GHz Band', September 1999
2 HYPERTEX http://stdsbbs.ieee.org/group/802/11
3 VEIT, W., FENK, J., GANSER, S., HADJIZADA, K., HEINEN, S., HERRMANN, H., and SEHRIG, P.: 'A 2.7 V 800 MHz-2.1 GHz transceiver chipset for mobile radio applications in 25 GHz f_t Si-bipolar'. Bipolar/BiCMOS Circuits and Technology Mtg, Minneapolis, MN, USA, October 1994, pp. 175–178
4 MEYER, R.G., MACK, W.D., and HAGERAATS, J.J.E.M.: 'A 2.5 GHz BiCMOS transceiver for wireless LAN'. Solid-State Circuits Conf., 1997, Dig. Tech. Pprs. 44th ISSCC., San Francisco, California, USA, pp. 310–311, 477
5 LI PUMA, G., GEPPERT, W., HADJIZADA, K., VAN WAASEN, S., MEVISSEN, W., VON SCHWARTZENBERG, W., and HEINEN, S.: 'An RF transceiver for WDCT in a 25 GHz Si bipolar technology', *IEEE MTT-S Int. Microw. Symp. Dig.*, 2000, **1**, pp. 1273–1276
6 TSENG, P.D., ZHANG, L., GAO, G.B., and CHANG, M.F.: 'A 3-V monolithic SiGe HBT power amplifier for dual-mode (CDMA/AMS) cellular handset applications', *IEEE J. Solid-State Circuits*, 2000, **35**, (9), pp. 1338–1344
7 BISCHOF, W., ALLES, M., GERLACH, S., KRUCK, A., SCHUPPEN, A., SINDERHAUF, J., and WASSENER, H.-J.: 'SiGe power amplifier in flipchip and packaged technology'. IEEE 2001 RFIC-S Dig., Phoenix, Arizona, USA, 2001, pp. 35–38
8 RAGHAVAN, A., HEO, D., MAENG, M., SUTONO, A., LIM, K., and LASKAR, J.: 'A 2.4 GHz high efficiency SiGe HBT power amplifier with high-Q LTCC harmonic suppression filter', *IEEE MTT-S Int. Microw. Symp. Dig.*, 2002, pp. 1019–1022
9 GOTZFRIED, R., BEISSWANGER, F., GERLACH, S., SCHUPPEN, A., DIETRICH, H., SEILER, U., BACH, K.-H., and ALBERS, J.: 'RFIC's for mobile communication systems using SiGe bipolar technology', *IEEE Trans. Microw. Theory Tech.*, 1998, **46**, (5), pp. 661–668
10 HYPERTEX http://www.austriamicrosystems.com/
11 ROULSTON, D.J.: 'Bipolar semiconductor devices' (McGraw Hill, 1990)
12 KOLDING, T.E.: 'Consistent layout techniques for successful RF CMOS design'. Proc. of Workshop on New Technologies for RF Circuits, March 2000. (Invited paper), Microwave Engineering Europe, Bracknell, UK, pp. 46–56

Tight approximation for coherent MPSK symbol error probability

Seungkeun Park, Dongweon Yoon and Kyungrok Cho

Many bounds for symbol error probability of MPSK have been used in the literature because a closed form expression that does not require a numerical integration for MPSK symbol error probability has not yet been derived. The bounds for MPSK symbol error probability used in the past are simple to calculate but inaccurate, or accurate but complex. A very simple and extremely tight new approximation is presented of symbol error probability for coherent MPSK.

Introduction: Symbol error probability and bit error probability have been used extensively as a fundamental measure of performance for an M-ary digital communication system. However, closed-form expressions for the symbol error rate (SER) or for the bit error rate (BER) of some two-dimensional modulation schemes, for example SER or BER for M-ary phase shift keying (MPSK), or SER or BER for circular quadrature amplitude modulation (QAM), have not yet been derived. Recently, Cho and Yoon [1] obtained an exact and generic closed-form expression for the BER of rectangular QAM. In this Letter, we investigate the SER for coherent M-ary PSK. The SER for coherent MPSK signals in AWGN is [2]

$$P(M) = 1 - \int_{-\pi/M}^{\pi/M} f(\theta)\, d\theta \qquad (1)$$

where $f(\theta)$ is the probability density function (pdf) of the phase fluctuation due to AWGN for M-ary PSK systems and is given by

$$f(\theta) = \sqrt{\frac{r}{\pi}} \cos\theta e^{-r\sin^2\theta} + \frac{e^{-r}}{2\pi}(1 - \sqrt{\pi r}\cos\theta e^{r\cos^2\theta}\mathrm{erfc}(\sqrt{r}\cos\theta)) \qquad (2)$$

where $\mathrm{erfc}(\cdot)$ is the complementary error function [3], and r is the signal-to-noise ratio (SNR) per symbol.

In general, (1) does not reduce to a closed form except when $M=2$ and $M=4$, and consequently upper and lower bounds on SER for MPSK ($M>4$) have been extensively used [4–7]. Very simple bounds are derived in [4] and [5], but these bounds are very loose. The bounds derived in [6] and [7] are much tighter than these. Chie [6] derived simple and tight upper and lower bounds by using asymptotic expansion, but these are not true bounds because they require the selection of the appropriate number of terms in an asymptotic expansion. More recently, to avoid the problem of [6], that is, 'the problem of the appropriate number of terms in an asymptotic expansion,' an alternating function bound was introduced [7]. Komo and Barnett [7] derived quite tight upper and lower bounds using a technique involving alternating functions to obtain even tighter bounds. The bounds in [7] are quite tight, but the expressions used are very complex. Specifically, the bounds of [7] have two constant terms that depend on numerical integration. In this Letter, a simple approximation on SER for MPSK with much tighter bound than [7] is derived and analysed. We use an asymptotic expansion as in [6], but the selection problem of the appropriate number of terms in the asymptotic expansion of [6] is not required.

New approximation: Here, a tighter approximation on $P(M)$ is developed by using the asymptotic expansion of the integrand in (1). Eqn. (1) becomes

$$P(M) = \mathrm{erfc}\left(\sqrt{r}\sin\left(\frac{\pi}{M}\right)\right) + C \qquad (3)$$

where

$$C = \int_{-\pi/M}^{\pi/M} \frac{e^{-r}}{2\pi}\left[\sqrt{\pi r}\cos\theta\, e^{r\cos^2\theta}\mathrm{erfc}(\sqrt{r}\cos\theta) - 1\right] d\theta \qquad (4)$$

is the correction term.

By using the asymptotic series expansion [3]

$$\sqrt{\pi}x e^{x^2}\mathrm{erfc}(x) \simeq 1 + \sum_{n=1}^{\infty}(-1)^n \frac{1\cdot 3\cdots(2n-1)}{(2x^2)^n} \qquad (5)$$

and after some manipulations, we obtain

$$C \approx \frac{e^{-r}}{\pi}\sum_{n=1}^{\infty}(-1)^n \frac{1\cdot 3\cdot 5\cdots(2n-1)}{(2r)^n}\int_0^{\pi/M}\frac{1}{\cos^{2n}\theta}\, d\theta \qquad (6)$$

Given that

$$\cos^{2n}(\theta) \le \cos^2(\theta), \quad \text{for } n = 1, 2, 3, \ldots \qquad (7)$$

the lower bound of (6) becomes

$$\begin{aligned} C &\ge \frac{e^{-r}}{\pi}\sum_{n=1}^{\infty}(-1)^n \frac{1\cdot 3\cdot 5\cdots(2n-1)}{(2r)^n}\int_0^{\pi/M}\frac{1}{\cos^2\theta}\, d\theta \\ &= \frac{e^{-r}}{\pi}\tan\left(\frac{\pi}{M}\right)\sum_{n=1}^{\infty}(-1)^n \frac{1\cdot 3\cdot 5\cdots(2n-1)}{(2r)^n} \end{aligned} \qquad (8)$$

By reusing the asymptotic series expansion of (5), the lower bound approximation of (8) can now be expressed as follows:

$$C \simeq \frac{e^{-r}}{\pi}\tan\left(\frac{\pi}{M}\right)\left[1 - \sqrt{\pi r}e^{r}\mathrm{erfc}(\sqrt{r})\right] \qquad (9)$$

Finally, substituting (9) into (3), an extremely tight approximation on $P(M)$ for $M>4$ is obtained as

$$\begin{aligned} P(M) \simeq{}& \mathrm{erfc}\left(\sqrt{r}\sin\left(\frac{\pi}{M}\right)\right) - \frac{e^{-r}}{\pi}\tan\left(\frac{\pi}{M}\right) \\ &+ \sqrt{\frac{r}{\pi}}\tan\left(\frac{\pi}{M}\right)\mathrm{erfc}(\sqrt{r}), \quad M > 4 \end{aligned} \qquad (10)$$